ISSN 1392 - 1207. MECHANIKA. 2009. Nr.6(80)

Low cycle stress strain curves and fatigue under tension-compression and torsion

M. Daunys*, R. Česnavičius**
**Kaunas University of Technology, Kęstučio 27, 44312 Kaunas, Lithuania, E-mail: mykolas.daunys@ktu.lt*
***Kaunas University of Technology, Kęstučio 27, 44312 Kaunas, Lithuania, E-mail: ramunas.cesnavicius@ktu.lt*

1. Introduction

During exploitation damage gradually appears in the constructions materials and results their fracture. The gradually accumulated damage depends on material properties, magnitude and character of the time-dependent stress and strain variation, environment conditions. It was observed, that 75 % of fracture in mechanical constructions is causes by the material fatigue. Especially dangerous are the overloads, as cyclically varying loading exceeds the proportionality limit of the material and causes plastic strain and formation of the hysteresis loop, while durability of the material decreases to thousands or hundreds of cycles [1]. In most mechanisms and devices under loading the elastic-plastic strain appears in stress concentration areas, near the sudden change of the shape, e.g. in key seats, near shafts diameter changing places, as a result of incorrectly chosen fillet radius, in welded joints, because of the various welding defects and etc. [2, 3]. Under cyclic elastic-plastic loading, after the cycle number of hundreds – thousands, the fatigue crack appears which commonly causes failures with hardly predictable outcome.

The problems of metal fracture remain actual despite years of long-lasting investigation of the cyclic loading of metals [4]. While selecting the material, it is necessary to know properties and change laws of their characteristics under different type loading in the areas of the periodically varying elastic-plastic strain. Most common are the following three types of loading: tension-compression, bending and torsion [5].

If compared to tension-compression and bending tests, the number of performed low cycle torsion loading tests is not so considerable. It should be noted, that a large amount of the parts in real operating conditions, i.e. shafts, springs and others parts of the mechanisms, are exactly under cyclically varying torsion loading [6, 7].

2. Experimental setup and used specimens

All performed experimental analyses: monotonous tension, monotonous torsion, low cycle tension-compression and low cycle torsion were carried out under ambient temperature. For both the mentioned cases, the specimens were under symmetric loading and experimental data was registered up to crack initiation.

For monotonous tension and low cycle tension-compression fatigue analysis the experimental low cycle setup, designed and made at Machine Design Department of the Kaunas University of Technology, was used. Experimental setup consists of 50 kN testing machine and an electronic part, which is designed to record the stress strain diagrams, semicycles and control the motor reversal.

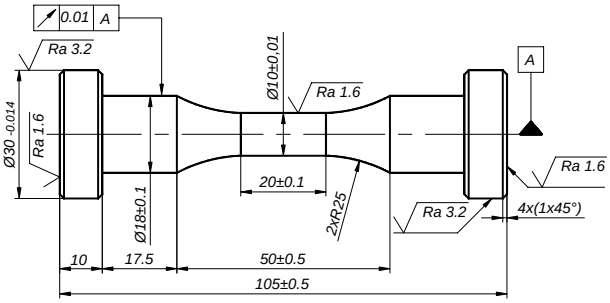

Fig. 1 Specimen for monotonous and low cycle tension-compression

The specimens of circular cross-section have been used for the monotonous tension and low cycle tension-compression experiments. The specimens were made of the grade 45 steel rods, following the dimensions presented in Fig. 1.

For the monotonous and low cycle torsion fatigue tests the experimental low cycle setup with T=500 Nm torgue and the same electronic equipment, as in tension-compression analysis, was used.

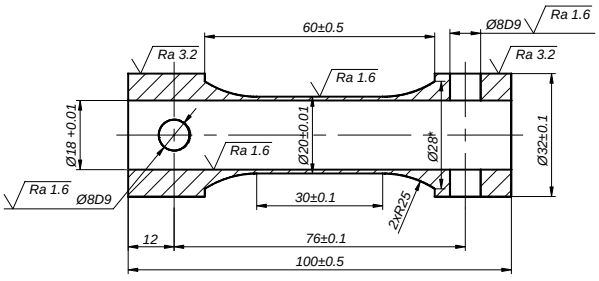

Fig. 2 Specimen for monotonous and low cycle torsion

Tubular shape specimens with t/d=1/20 working part were used for the experiments. The specimen is shown in Fig. 2. During the cyclic torsion uniform stress state is produced within the wall of the tubular specimen, i.e. the stress gradient does not have the influence. To fulfil the working part of the test, the same fillet radius R = 25 mm was used for both the torsion and tension-compression specimens, aiming to decrease the stress concentration to minimum (the theoretical stress concentration coefficient $\alpha_\sigma \approx 1.03$).

To determine the torque T, resistance wire gauges were glued on the surface of the device with cylindrical working part d=18.0 mm. This device is made of the thermal treatmed grade 60S2A spring steel (HRC 42-45). The working strain gauges were glued to the cylinder's surface along the main strain directions e_1 and e_3 (at 45º angle, in opposite sides).

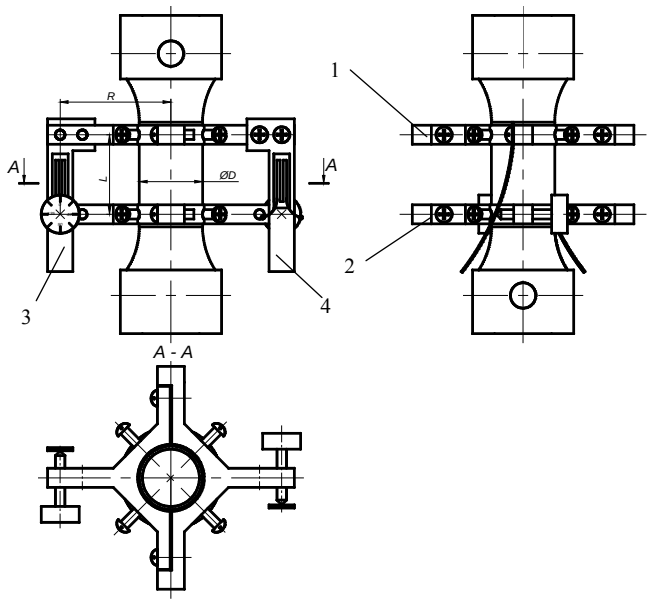

Fig. 3 Tenzometer for torsion angle measurements

The torsion strain is measured by the attachment, which identifies the torsion angle φ in the working part of the specimen. The device for torsion angle measurements, presented in Fig. 3, consists of two rings *1* and *2*, each of them has bolt fastened half rings, that are attached to the specimen by means of the 4 conical tip bolts, locating them at identical angles. Two spring steel plates *3* and *4* are fastened to the top ring. Working gauges (R=100 Ω) are glued along tension-compression sides of the plates. Free end of each plate rests on bolt-adjusted bottom retainer ring. During torsion of the specimen, the rings turn relative to each other and sprung steel plates act as cantilever rods during bending.

3. Experimental analysis

3.1. Investigation of the monotonous loading

During the experiments of monotonous loading, the monotonous tension and monotonous torsion curves were obtained. The curves of the monotonous tension and torsion in coordinates σ_i - e_i, and $\tau_{max} - \gamma_{max}$ are presented in Figs. 4 and 5. The determined mechanical characteristics of the grade 45 steel under tension are given in Table 1 and under torsion – in Table 2.

The curves of monotonous tension in σ_i - e_i coordinates were obtained applying the equalities

$$\sigma_i = \sigma_1 ;\ e_i = e_1 \qquad (1)$$

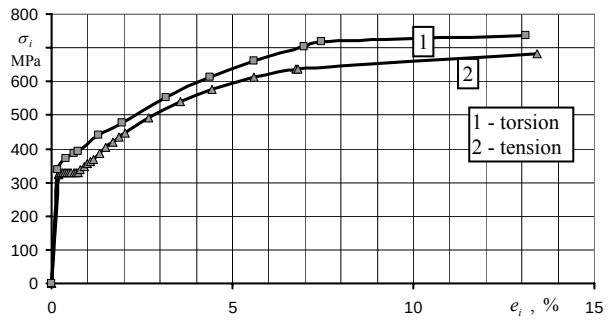

Fig. 4 Curves of the monotonous tension and torsion

The curves of monotonous torsion in σ_i - e_i coordinates were obtained by the Eqs. 2.

$$\sigma_i = \sqrt{3}\tau ;\ e_i = \frac{\gamma}{\sqrt{3}} \qquad (2)$$

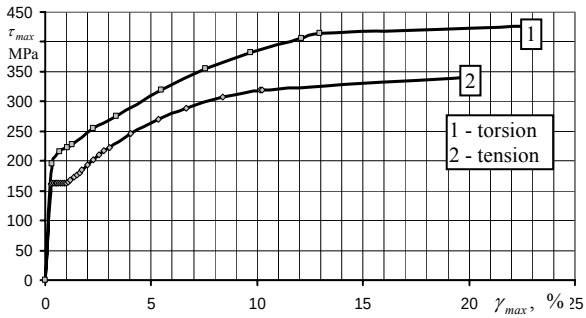

Fig. 5 Curves of monotonous tension and torsion

The curves of monotonous tension in $\tau_{max} - \gamma_{max}$ coordinates were obtained by

$$\tau_{max} = \frac{\sigma_1}{2} ;\ \gamma_{max} = 1.5e_1 \qquad (3)$$

The curves of monotonous torsion in $\tau_{max} - \gamma_{max}$ coordinates were obtained by the Eq. 4.

$$\tau_{max} = \tau ;\ \gamma_{max} = \gamma \qquad (4)$$

It is seen from the Figs. 4 and 5 that monotonous tension and torsion curves in σ_i - e_i coordinates are closer than the same curves in $\tau_{max} - \gamma_{max}$ coordinates.

Table 1

Mechanical characteristics of the grade 45 steel under tension

σ_{pl}, MPa	$\sigma_{0.2}$, MPa	σ_u, MPa	σ_f, MPa	e_{u2}, %	ψ, %
319	320	673	1000	13.1	43.8
325	334	686	993	12.5	37.6
324	328	688	995	13.0	40.6
$\bar{x}$					
323	327	682	996	12.9	40.7

Table 2

Mechanical characteristics of the grade 45 steel under torsion

τ_{pl}, MPa	$\tau_{0.3}$, MPa	τ_u, MPa	γ_{u2}, %
174	226	425	23.4
224	209	435	25.2
188	211	420	19.7
$\bar{x}$			
195	215	426	22.7

3.2. Low cycle stress strain curves

Under stress limited low cycle loading, the determined hysteresis loop width dependence both on the number of loading semicycles k and loading level $\bar{\sigma}_0$, is presented in Fig. 6. The mentioned data was obtained during the tension-compression experiments, using loading levels from $\bar{\sigma}_0 = 1.08$ to $\bar{\sigma}_0 = 1.93$, where

$$\bar{\sigma}_0 = \frac{\sigma_0}{\sigma_{pl}};\ \bar{\delta}_k = \frac{\delta_k}{e_{pl}} \tag{5}$$

here σ_0 is loading stress amplitude, δ_k is width of the hysteresis loop of plastic strain for loading semicycle k, σ_{pl} and e_{pl} are stress and strain of proportionality limit [1].

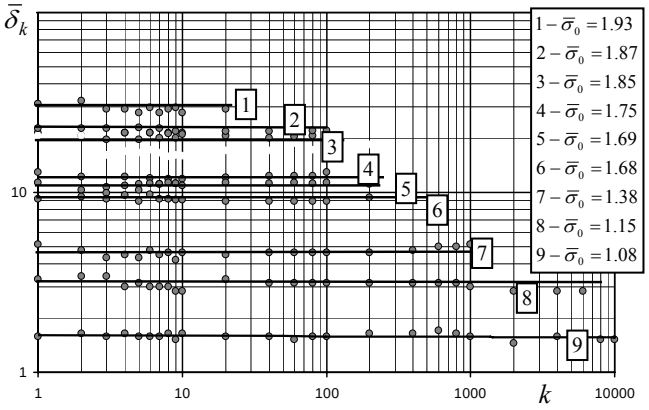

Fig. 6 Hysteresis loop width dependence both on the number of loading semicycles k and loading level $\bar{\sigma}_0$ for grade 45 steel under tension-compression

Fig. 6 shows, that at increasing the number k of the loading semicycles, the hysteresis loop's width $\bar{\delta}$ for grade 45 steel is not changing, i.e. remains constant, consequently we have stable material.

Low cycle torsion stress limited loading experiments were carried out using the loading levels from $\bar{\tau}_0 = 1.12$ to $\bar{\tau}_0 = 1.94$. Fig. 7 shows, that increasing the number of loading semicycles k for the grade 45 steel hysteresis loop width $\bar{\delta}$ is not changing as under tension-compression, i.e. it remains constant.

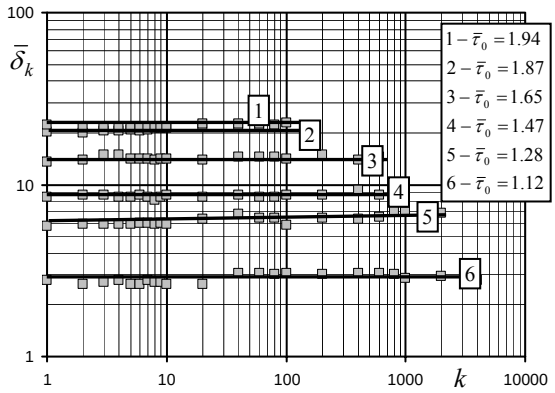

Fig. 7 Hysteresis loop width dependence on the number of loading semicycles k and loading level $\bar{\tau}_0$ for grade 45 steel under torsion low cycle loading

Width of the hysteresis loop during tension-compression for the cyclic anisotropic materials is wider at even semicycles and smaller at uneven, i.e. $\bar{\delta}_{even} > \bar{\delta}_{uneven}$. For the case of torsion, the width of the hysteresis loop remains constant. Therefore, the hysteresis loop width dependence on the number of semicycles is written as follows [1]

$$\bar{\delta}_k = A_{1,2}\left(\bar{e}_0 - \frac{\bar{s}_T}{2}\right)k^{\alpha} \tag{6}$$

where A_1, A_2 and α are cyclic characteristics of the material, $\bar{e}_0$ is relative initial strain, $\bar{s}_T$ is cyclic proportionality limit.

To determine tension-compression constants A_1 and A_2, and torsion constant A under stress limited low cycle loading, $\bar{\delta}_{1,2} = f(\bar{e}_0)$ graphs of the semicycle hysteresis loop width dependence on initial strain have been used [1], i.e.

$$A_{1,2} = \frac{\bar{\delta}_{1,2}}{\left(\bar{e}_0 - \frac{\bar{s}_T}{2}\right)} \tag{7}$$

Dependences of semicycle's loop width on the initial strain are shown in Figs. 8 and 9, whereas determined cyclic characteristics of the material are given in Table 3.

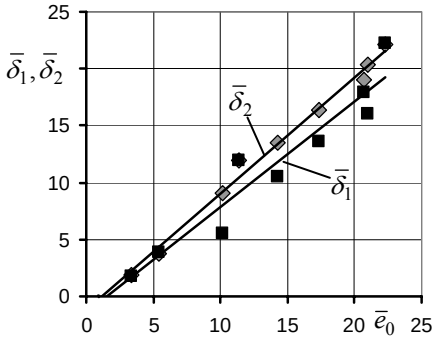

Fig. 8 Dependence of the hysteresis loop width on the initial strain of grade 45 steel under low cycle tension-compression for the first and second loading semicycles

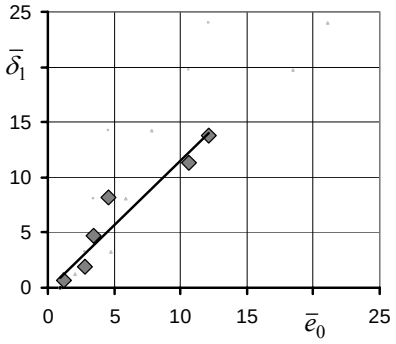

Fig. 9 Dependence of the first semicycle hysteresis loop's width on initial strain for grade 45 steel under low cycle torsion

Table 3

Cyclic characteristics of the grade 45 steel

Tension-compression				Torsion		
A_1	A_2	$\bar{s}_T$	α	A	$\bar{s}_T$	α
Grade 45 steel						
0.93	1.01	1.65	0	1.14	1.40	0

Carrying out the low cycle tension-compression tests, it was obtained, that grade 45 steel is accumulating

plastic strain in tension direction (Fig. 10). Thus, the accumulated plastic strain after loading semicycles k, can be expressed as follows [1]

$$\bar{e}_{pk} = \bar{e}_0 - \bar{\sigma}_0 + \sum_1^k (-1)^k \ \bar{\delta}_k \qquad (8)$$

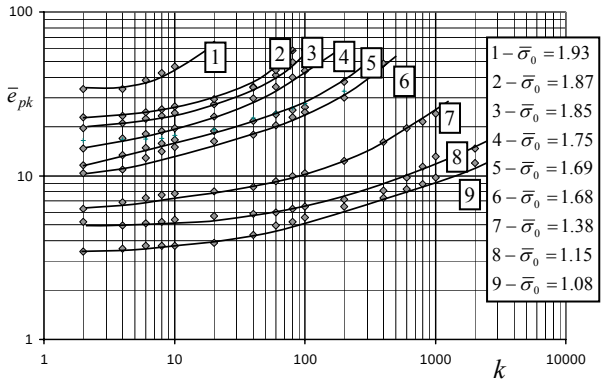

Fig. 10 Curves of accumulated plastic strain $\bar{e}_{pk}$ till crack initiation, under stress limited tension-compression, depending on the number of semicycles k and loading level $\bar{\sigma}_0$

Carrying out the low cycle torsion tests, it was obtained, that grade 45 steel does not accumulate plastic strain.

3.2. Low cycle fatigue curves

Fig. 11 presents curves of low cycle fatigue and reduction of area ψ for grade 45 steel under stress limited tension-compression loading.

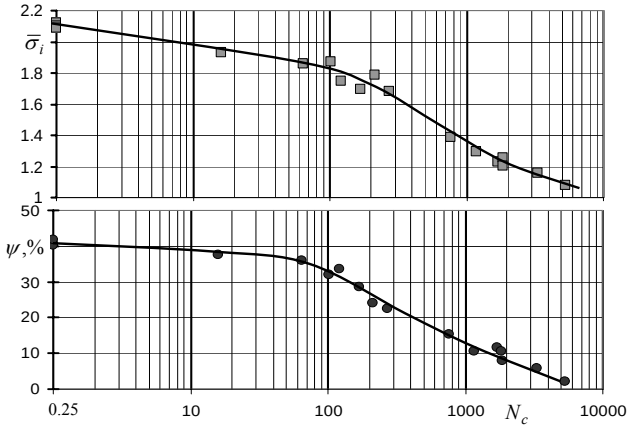

Fig. 11 Curves of low cycle fatigue and reduction of the area of cross-section ψ under stress limited tension-compression

Fig. 12 presents low cycle fatigue curves of grade 45 steel under stress limited torsion.

Under strain limited low cycle loading, the accumulation of plastic strain $\bar{e}_{pk}$ is not available. Experimental analysis of low cycle strain limited loading was carried out at tension-compression levels from $\bar{e}_{0min} = 3.42$ to $\bar{e}_{0max} = 16.15$ and for the torsion levels – from $\bar{e}_{0min} = 4.56$ to $\bar{e}_{0max} = 19.63$. Figs. 13 and 14 present low cycle fatigue curves under strain limited loading in coordinates $lg\,\bar{\delta} - lg\,k_c$ and $lg\,\bar{\varepsilon} - lg\,k_c$.

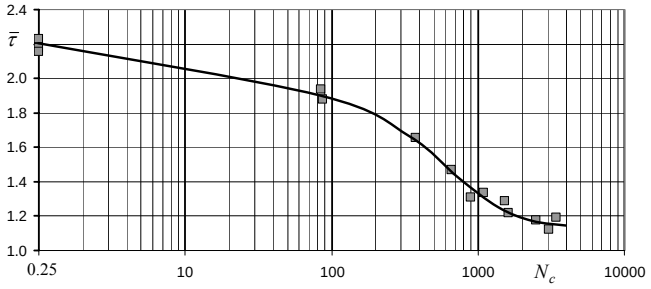

Fig. 12 Low cycle fatigue curve under stress limited torsion loading

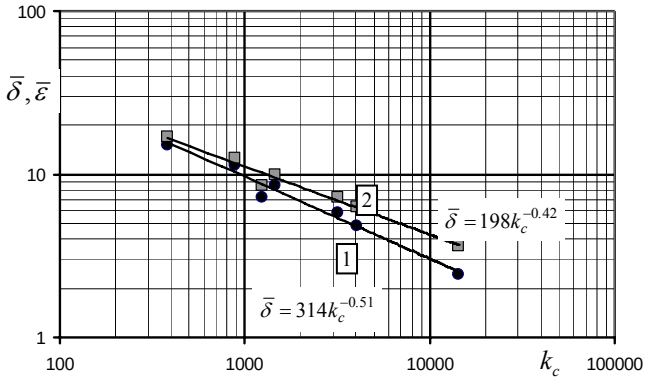

Fig. 13 Fatigue curves of grade 45 steel under strain limited tension-compression: *1* – in coordinates $lg\,\bar{\delta} - lg\,k_c$; *2* – in coordinates $lg\,\bar{\varepsilon} - lg\,k_c$

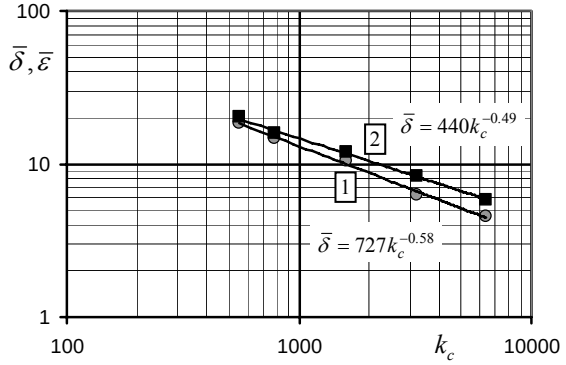

Fig. 14 Fatigue curves of grade 45 steel under strain limited torsion: *1* – in coordinates $lg\,\bar{\delta} - lg\,k_c$; *2* – in coordinates $lg\,\bar{\varepsilon} - lg\,k_c$

Table 4

Values of Coffins constants C and m

Steel 45				
C_2	C_3	m_1	m_2	m_3
Low cycle tension-compression				
314	198	0.42	0.51	1.14
Low cycle torsion				
727	440	0.49	0.58	0.88

4. Damage under low cycle loading

Under tension-compression and stress limited loading, fracture of the specimen occurs due to quasistatic

damage d_K, caused by the accumulated plastic strain $\bar{e}_{pk}$, and fatigue damage d_N, caused by the cyclic plastic strain, which is caused by the hysteresis loop width $\bar{\delta}_k$, whereas total damage may be written [1]

$$d = d_K^q + d_N^l \tag{9}$$

where d is total damage.

Fatigue damage is calculated by the equation

$$d_N = \frac{\sum_1^k \bar{\delta}_k}{\sum_1^{k_c} \bar{\delta}_k} \tag{10}$$

where $\sum_1^k \bar{\delta}_k$ is fatigue damage accumulated during the k loading semicycles, $\sum_1^{k_c} \bar{\delta}_k$ is fatigue damage accumulated till crack initiation.

Quasistatic damage

$$d_K = \frac{\bar{e}_{pl}}{\bar{e}_{u_2}} \tag{11}$$

where $\bar{e}_{pl}$ is accumulated plastic strain during k semicycles of loading, whereas $\bar{e}_{u_2}$ is the maximum uniform strain under monotonous loading which corresponds σ_u.

If stress limited loading is approached as non-stationary strain limited loading, when the damage, accumulated during one semicycle k, is expressed as

$$d_N = \frac{\bar{\delta}_k}{\sum_1^{k_c} \bar{\delta}_k} \tag{12}$$

Then condition of the crack initiation is

$$\frac{\bar{\delta}_1}{\sum_1^{k_{c1}} \bar{\delta}_k} + \frac{\bar{\delta}_2}{\sum_1^{k_{c2}} \bar{\delta}_k} + \ldots + \frac{\bar{\delta}_c}{\sum_1^{k_{ck_c}} \bar{\delta}_k} = 1 \tag{13}$$

The analysis of strain limited low cycle loading when strain is limited and quasistatic damage is not occurring was performed. In this case, damage of the specimen is predetermined only by the cyclic plastic strain, i.e. under strain limited loading, the fatigue curve in coordinates $lg\,\bar{\delta} - lg\,k_c$ has a shape of straight line. The constants m and C have been determined by the equation of straight line

$$lg\,\bar{\delta} = -m\,lg\,k_c + lg\,C \tag{14}$$

or

$$\bar{\delta}\, k_c^m = C \tag{15}$$

where $\bar{\delta}$ is average width of the hysteresis loop.

From the fatigue curve, formed under strain limited loading, in coordinates $lg\,\bar{\delta} - lg\,k_c$ and $lg\,\bar{\varepsilon} - lg\,k_c$ and applying the L.Coffin's equation

$$\bar{\delta}_m = C_2 k_c^{-m_2} \tag{16}$$

In expression (16), the average width of the plastic hysteresis loop was calculated by the equation:

$$\bar{\delta}_m = \frac{1}{k_c} \sum_1^{k_c} \bar{\delta}_k \tag{17}$$

therefore

$$\sum_1^{k_c} \bar{\delta}_k = C_2 k_c^{1-m_2} \tag{18}$$

Applying the coordinates $lg\,\bar{\varepsilon} - lg\,k_c$, we obtain

$$\bar{\varepsilon} k_c^{m_1} = C_3 \tag{19}$$

and

$$k_c = \frac{C_3^{1/m_1}}{\bar{\varepsilon}^{1/m_1}} \tag{20}$$

After the applied Eq. (20)

$$\sum_1^{k_c} \bar{\delta}_k = C_2 \frac{C_3^{1-m_2/m_1}}{\bar{\varepsilon}^{1-m_2/m_1}} \tag{21}$$

By introducing the $m_3 = 1 - m_2/m_1$ and applying the Eqs. (13) - (21), we obtain

$$\frac{\bar{\delta}_1 \bar{\varepsilon}_1^{m_3}}{C_2 C_3^{m_3}} + \frac{\bar{\delta}_2 \bar{\varepsilon}_2^{m_3}}{C_2 C_3^{m_3}} + \ldots + \frac{\bar{\delta}_{k_c} \bar{\varepsilon}_{k_c}^{m_3}}{C_2 C_3^{m_3}} = 1 \tag{22}$$

Because of good agreement between the experimental and calculated data, Eq. (22) was used to calculate the damage in works [8, 9].

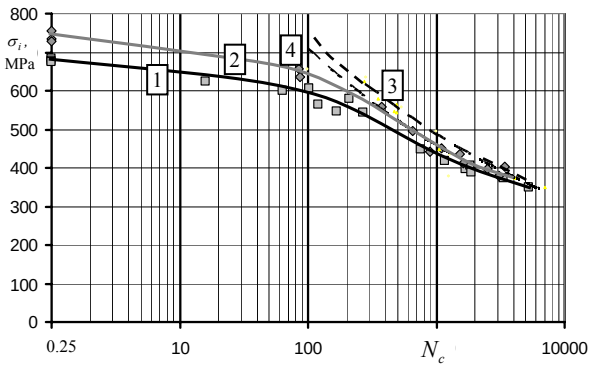

Fig. 15 Curves of low cycle fatigue under stress limited loading, respectively: *1* – tension-compression, *2* – torsion, *3* – theoretical curve of the tension-compression, when only fatigue damage is taken into account, *4* – theoretical curve of the torsion, as only fatigue damage is taken into account

The curve *3* in Fig. 15 presents the fatigue damage under stress limited tension-compression as only fatigue damage is taken into account and is close to the fatigue curve under stress limited torsion (curve *2*), because under stress limited torsion loading, strain accumulation is not observed, i.e., the quasistatic damage does not occur.

The curve *4* confirms Eq. (22), as it shows satisfactory agreement to fatigue curve under stress limited torsion, because during the torsion experiments the quasistatic damage was not observed. The curves *3* and *4* confirm that according to the results of cyclic tension-compression it is possible to calculate the durability under cyclic torsion. Besides, the durability under cyclic torsion (in coordinates σ_i - N_c) is higher than under cyclic tension-compression loading, because under cyclic torsion there is no accumulation of plastic strain, i.e. there is no quasistatic damage.

5. Conclusions

Grade 45 steel was investigated under monotonous tension, monotonous torsion, the low cycle tension-compression and low cycle torsion with stress and strain limited loading, using the circular cross-section specimens for tension-compression and thin walled specimens – for torsion.

1. It was determined, that characteristics of the cyclic stress strain curves for the analyzed grade 45 steel at cyclic tension-compression, and under cyclic torsion, are similar. For both the analyzed loading cases the parameter $\alpha = 0$, i.e. the material is cyclically stable. Values of the parameters A, which characterizes the hysteresis loop width of the first semicycle, are also similar.

2. During the stress limited loading, under cyclic torsion, the accumulation of plastic strain was not observed, i.e. under stress limited torsion, there is no quasistatic damage.

3. The durability under cyclic torsion is higher (in coordinates σ_i - N_c), than that under cyclic tension - compression loading, because under cyclic torsion there is no accumulation of plastic strain, i.e. is no quasistatic damage.

References

1. **Daunys, M.** Cycle Strength and Durability of Structures. -Kaunas: Technologija, 2005. -286p. (in Lithuanian).
2. **Krenevičius, A., Leonavičius, M**. Fatigue life prediction for threaded joint. -Mechanika, -Kaunas: Technologija, 2008, Nr.3(71), p.5-11.
3. **Krenevičius, A., Juchnevičius, Ž**. Load distribution in the threaded joint subjected to bending. -Mechanika, -Kaunas: Technologija, 2009, Nr.4(78), p.12-16.
4. **Findley, WN.** Effects of extremes of hardness and mean stress on fatigue of AISI steel in bending and torsion. -ASME Journal of Engineering Materials and Technology, 1989, p.119-122.
5. **Shigley, JE., Mischke, CR.** Mechanical Engineering Design, 5th ed. -McGraw-Hill, 1989.-1018p.
6. **Marquis, G., Socie, D.** Long-life torsion fatigue with normal mean stresses. -Fatigue and Fracture of Engineering Materials and Structures, 2000, p.293-300.
7. **McClaflin, D., Fatemi, A.** Torsional deformation and fatigue of hardened steel including mean stress and stress gradient effects. -International Journal of Fatigue. –Elsevier, 2004, 26, p.773-784.
8. **Daunys, M., Rimovskis, S.** Analysis of circular cross-section element, loaded by static and cyclic elastic-plastic pure bending. -International Journal of Fatigue. -Elsevier, 2006, 28, p.211-222.
9. **Daunys, M., Sabaliauskas, A**. Influence of surface hardening on low cycle tension compression and bending characteristics. -Mechanika. -Kaunas: Technologija, 2005, Nr.3(53), p.12-16.

M. Daunys, R. Česnavičius

MAŽACIKLIO DEFORMAVIMO IR SUIRIMO KREIVĖS ESANT TEMPIMUI-GNIUŽDYMUI IR SUKIMUI

R e z i u m ė

Straipsnyje nagrinėjamas plieno 45 mažaciklis nuovargis esant apribotiems įtempiams ir deformacijoms bei tempimui-gniuždymui ir sukimui.

Nustatyta, kad tiriamoji medžiaga yra ciklišk ai stabili tiek tempiama bei gniuždoma, tiek sukama (parametras α=0), o deformavimo diagramų forma abiem apkrovimo atvejais yra panaši, nes parametrai A yra panašūs tiek esant tempimui bei gniuždymui, tiek sukimui. Ciklinio sukimo metu, esant apkrovimui su apribotais įtempiais, vienpusė plastinė deformacija nekaupiama, t. y nėra kvazistatinių pažeidimų. Straipsnyje panaudotos analitinės priklausomybės nuovargio pažeidimams apskaičiuoti gerai tenkina ciklinio sukimo duomenis, nes teorinė ciklinio sukimo nuovargio kreivė gerai sutampa su eksperimentine kreive, gauta esant apribotiems įtempiams, ir yra artima teorinei ciklinio tempimo bei gniuždymo nuovargio kreivei įvertinančiai tik nuovargio pažeidimus esant apkrovai su apribotais įtempiais.

Tai rodo, kad, esant cikliniam sukimui, ilgalaikiškumas (koordinatėse $\sigma_i - N_c$) yra didesnis už ilgalaikiškumą esant cikliniam tempimui bei gniuždymui, nes šiuo atveju plastinė deformacija nekaupiama t. y. nėra kvazistactinių pažeidimų.

M. Daunys, R. Česnavičius

LOW CYCLE STRESS STRAIN CURVES AND FATIGUE UNDER TENSION-COMPRESSION AND TORSION

S u m m a r y

The presented paper analyses low cycle fatigue of the grade 45 steel under stress and strain controlled low cycle tension-compression and torsion.

It was determined, that analysed material is cyclically stable, in both the tension-compression and torsion cases, because the parameter $\alpha = 0$. The shape of the stress strain diagrams for both the analysed loading cases is similar, as parameters A are similar for the tension-compression and the torsion. During the cyclic torsion, under stress limited loading, the accumulation of plastic strain is not ob-

served, i.e. quasistatic damage does not occur. The analytical dependences applied for the fatigue damage calculation showed good agreement with the cyclic torsion data, since the theoretical fatigue curve for cyclic torsion showed good agreement with the experimental curve for the stress limited case – and is close to the theoretical fatigue curve under stress limited cyclic tension-compression loading, when estimating only fatigue damage.

This shows, that under cyclic torsion, the durability (in $\sigma_i - N_c$ coordinates) is higher than the durability under cyclic tension-compression, because in this case the plastic strain is not accumulated, i.e. the quasistatic damage does not occur.

М. Даунис, Р. Чеснавичюс

КРИВЫЕ МАЛОЦИКЛОВОГО ДЕФОРМИРОВАНИЯ И РАЗРУШЕНИЯ ПРИ РАСТЯЖЕНИИ-СЖАТИИ И КРУЧЕНИИ

Р е з ю м е

В статье представлен анализ результатов малоцикловой усталости стали 45 при ограниченных напряжениях и деформациях, в условиях растяжения-сжатия и кручения.

Установлено, что исследованный материал является циклически стабильным при растяжении-сжатии и кручении (параметр $\alpha = 0$) и для обоих случаев нагрузки диаграммы деформирования близки по форме, в связи с тем, что значения параметров A для обоих случаев нагрузки отличаются мало. При циклическом кручении с ограниченным моментом кручения отсутствует накопление односторонней пластической деформации, т. е. нет квазистатических повреждений. Аналитические зависимости, использованные для расчета усталостных повреждений, дали хорошую сходимость с данными циклического кручения, так как теоретическая усталостная кривая хорошо сходится с экспериментальной кривой кручения при ограниченных напряжениях и близка к теоретической усталостной кривой при циклическом растяжении-сжатии, когда при нагрузке с ограниченными напряжениями учитываются только усталостные повреждения.

Полученные результаты показывают, что долговечность (в координатах $\sigma_i - N_c$) при циклическом кручении больше, чем долговечность при циклическом растяжении-сжатии, так как в случае кручения отсутствует накопление пластической деформации, т. е. нет квазистатических повреждений.

Received September 29, 2009
Accepted November 23, 2009